A simple and versatile analytical approach for planar metamaterials

Jörg Petschulat,* Arkadi Chipouline, Andreas Tünnermann,† and Thomas Pertsch
Institute of Applied Physics, Friedrich-Schiller-Universität Jena, Max Wien Platz 1, 07743 Jena, Germany

Christoph Menzel, Carsten Rockstuhl, Thomas Paul, and Falk Lederer
Institute of Condensed Matter Theory and Solid State Optics,
Friedrich-Schiller-Universität Jena, Max Wien Platz 1, 07743 Jena, Germany
(Dated: January 11, 2010)

We present an analytical model which permits the calculation of effective material parameters for planar metamaterials consisting of arbitrary unit cells (metaatoms) formed by a set of straight wire sections of potentially different shape. The model takes advantage of resonant electric dipole oscillations in the wires and their mutual coupling. The pertinent form of the metaatom determines the actual coupling features. This procedure represents a kind of building block model for quite different metaatoms. Based on the parameters describing the individual dipole oscillations and their mutual coupling the entire effective metamaterial tensor can be determined. By knowing these parameters for a certain metaatom it can be systematically modified to create the desired features. Performing such modifications effective material properties as well as the far field intensities remain predictable. As an example the model is applied to reveal the occurrence of optical activity if the split ring resonator metaatom is modified to L- or S-shaped metaatoms.

PACS numbers: 78.20.Ek, 41.20.Jb, 42.25.Ja
Keywords: Metamaterials, Optical activity, Chirality

I. INTRODUCTION

Metamaterials extend the optical effective material response of natural media. They are artificial materials that allow to tailor light propagation properties by a careful design of the mesoscopic metaatoms the metamaterial is made of. By controlling the geometry and selecting the material dispersion of the metaatom, novel effects such as negative refraction[1–3], optical cloaking[4–9], as well as a series of optical analogues to phenomena known from different disciplines in physics have been observed[10–14].

In principle, the material response is mathematically best described in terms of constitutive relations; leading to tensors that relate the electric displacement and the magnetic induction to the electric and magnetic fields, respectively. In the initial stage of research on metamaterials emphasize was put on exploring materials that potentially lead to a bi-axial anisotropic (linear dichroism) effective material response[1–3,15–17]. Recently research was also extended towards the exploration of metaatoms that affect off-diagonal elements of the effective material tensors (elliptical dichroism). It expands the number of observable optical phenomena, leading to, e.g., optical activity[18–22], bidirectional and asymmetric transmission[23–25] or chirality-induced negative refraction[26–28].

In our understanding optical activity comprises all effects on light propagation resulting from the nonlinearity of the polarization eigenstates, hence including phenomena like circular dichroism, all effects of genuine three-dimensional chirality and the optical manifestations of planar chirality[25].

However, despite the option to resort to rigorous computations for describing the light propagation on the mesoscopic level of the metaatoms, an enduring issue in metamaterial research is the question how the effective material tensor looks like for a certain metamaterial.

In general, investigating the geometry of the metamaterial (the metaatoms geometry *and* their arrangement) allows to determine the form of the effective material tensors in the quasi-static limit as extensively discussed in Ref. 19. From such considerations it is possible to conclude on the symmetry of the plasmonic eigenmodes sustained by the metaatoms and on the polarization of the eigenmodes allowed to propagate in the effective medium[23]. But in order to determine the actual frequency dependence of the tensor elements, more extended models are needed which start in their description of the metaatom properties from scratch[25]. Such models are required to be universal, simple and assumption-free to the largest possible extent.

Here we outline an approach which meets these requirements. It is based on conceptually decomposing the complex metatoms into a set of coupled plasmonic entities that sustain the excitation of dipolar resonances[29]. The knowledge of the plasmonic properties of these dipoles and their coupling suffices to derive the material response and the symmetry of the eigenmodes. This, in turn, permits to predict the observable quantities in the far-field, such as the polarization and frequency-dependent reflected and transmitted complex amplitudes.

The most appealing aspect of our model is that once the plasmonic entities and their coupling strengths are characterized, far-field properties remain predictable by the analytical model even if substantial modifications of the metaatom geometry have been made. Even a modification that leads to a different symmetry of the ma-

terial tensor does not prevent a quantitative description of the dispersive behavior of the tensor elements. To become specific, we start our investigations with an optical inactive, bi-axial anisotropic metamaterial, namely the split-ring resonator (SRR). From the observable far-field quantities we derive the properties of the dipolar oscillators that govern the plasmonic response of the three wires forming the SRR, namely the individual eigenfrequencies, oscillator strengths and damping constants as well as their mutual coupling strengths. By relying on these quantities, we determine the effective properties of metamaterials consisting of modified metaatoms with respect to the initial SRR.

We focus on two modifications that evoke optical activity. With our analytical model we predict the effective properties of these metamaterials. We then compute the optical coefficients for a slab made of these metamaterials and compare it to rigorous simulations. Excellent agreement between the analytically predicted and the rigorously calculated optical coefficients is observed throughout our work. Therefore, the proposed method can be used for the parameter retrieval without resorting to rigorous simulations. And since it is based on analytical considerations the approach potentially allows a large variety of metaatom modifications and to systematically tailor its effective properties. Hence our approach provides a powerful and versatile tool for a systematic analysis of achievable material properties by varying only a few constituents that may couple in some well-defined ways.

Furthermore, we will also show that such an analytical treatment provides further insight into metamaterial properties. Specifically, we show that it is possible to directly infer that the model's predictions are valid in terms of the Casimir-Onsager relations[30,31], the requirement for time-reversal and reciprocity in linear media[32].

Thus, the main aspects of the paper can be summarized as follows. At first, the localized carrier dynamics occurring in metaatoms may be properly described by a set of coupled oscillators, representing the decomposition of the metaatom in nanowire pieces. Second, the dynamics of these oscillators, determined by the shape of the nanowires and their coupling, result in electric dipole polarizabilities that permit the calculation of the effective permittivity tensor. The main advantage of this simple approach is that modifications of a metaatom, for which the oscillator dynamics and parameters have been found, leave the effective permittivity tensors predictable. Hence, the far field reflectance and transmittance can be calculated. We will show that this holds also for modifications changing the character of the eigenstates from linear to non-linear polarized. Moreover, the approach can be useful to determine the effective permittivity tensor for optically active metamaterials, whose eigenstates are in general elliptically polarized, by intensity measurements of linearly polarized light.

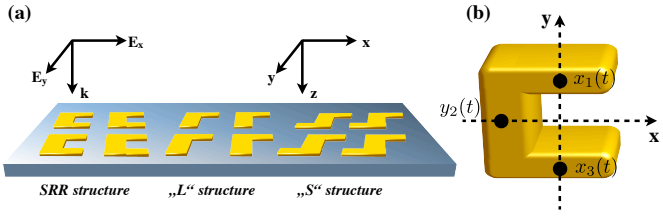

FIG. 1. (Color online) (a) The original SRR structure (left), the first modification, namely the L- (center) and the second modification, the S-structure (right). (b) The SRR together with the carrier oscillators, marked by black dots, which are used to phenomenologically replace the SRR.

II. THE PLANAR SRR METAATOM

To reveal the versatile character of our approach we will directly start by conceptually replacing the planar SRR geometry, shown in Fig. 1(b), by a set of coupled oscillators. Each of the oscillators introduced here represents a metaatoms piece, i.e. a straight nanowire that is coupled to its electrically conductive neighbors. The oscillators accounting for the isolated nanowire are associated with the excitation of carriers representing the free-electron gas of the metal. Hereby the carrier dynamics is solely influenced by the external electromagnetic field, including contributions from adjacent nanowires. The dynamics becomes resonant for the eigenfrequency of the localized plasmon polariton resonance of the individual nanowire. This localized resonance described by the individual oscillator corresponds to the fundamental electric dipole mode since the dimensions of the nanowires forming the metaatom investigated here are small compared with the wavelength. We will show later that the carrier oscillations of metaatoms assembled from several coupled wires still correspond to electric dipole polarizabilities. This holds as long as the wires are assembled in-plane. For out-of-plane structures higher order multipoles come generally into play[29,33].

Here the spatial coordinate represents the elongation of a negatively charged carrier density driven by an external electromagnetic field, which is the usual assumption in plasmonics[34].

We show below that this assumption is sufficient to entirely predict the optical response. The equations for the coupled oscillators are

$$\begin{aligned}
\frac{\partial^2}{\partial t^2}x_1 + \gamma_1\frac{\partial}{\partial t}x_1 + \omega_{01}^2 x_1 + \sigma_{21}y_2 &= -\frac{q_1}{m}E_x,\\
\frac{\partial^2}{\partial t^2}y_2 + \gamma_2\frac{\partial}{\partial t}y_2 + \omega_{02}^2 y_2 + \sigma_{21}x_1 - \sigma_{23}x_3 &= -\frac{q_2}{m}E_y,\\
\frac{\partial^2}{\partial t^2}x_3 + \gamma_3\frac{\partial}{\partial t}x_3 + \omega_{03}^2 x_3 - \sigma_{23}y_2 &= -\frac{q_3}{m}E_x,
\end{aligned} \tag{1}$$

where we have assumed nearest neighbor coupling between adjacent, i.e. conductively coupled dipolar oscillators. The oscillators are driven by the electric field

component of an external illuminating field propagating in z direction (normal incidence is assumed throughout the entire manuscript). Excitation of the oscillators by magnetic field components can be safely neglected[29,35]. In Eqs. (1) γ_j

is the damping, ω_{0j} the eigenfrequency, σ_{ij} the coupling constant and q_j is the charge for the three oscillators $(i,j) \in (1,2,3)$, respectively, similarly to those introduced in Ref. 29. The coordinates (x_1, y_2, x_3) themselves are understood as the displacement of the negatively charged carriers representing oscillating currents or multipole moments where both approaches can be used to determine the effective material response of an artificial medium exhibiting a carrier dynamics as described by Eq. (1)[36]. Here we apply the multipole approach to map the displacement onto electric dipole moments, since this is consistent with our previous works[29,33].

Accounting for the contributions of the electric dipole and quadrupole as well as the magnetic dipole moment the wave equation reads as

$$\begin{aligned}\Delta\mathbf{E}(\mathbf{r},\omega) = &-\mu_0\epsilon_0\omega^2\mathbf{E}(\mathbf{r},\omega) - \omega^2\mu_0\mathbf{P}(\mathbf{r},\omega)\\ &+\omega^2\mu_0\nabla\cdot\mathbf{Q}(\mathbf{r},\omega) - i\omega\mu_0\nabla\times\mathbf{M}(\mathbf{r},\omega),\end{aligned} \tag{2}$$

We put emphasis on the fact that the higher order multipole moments, leading to $\mathbf{Q}, \mathbf{M}$, appear in general[37], but do not provide any contribution in the present configuration, as mentioned above. Thus, there is no effective magnetic response (effective permeability tensor) as expected and it is sufficient to consider the dispersion in the susceptibility, resulting in a linear effective permittivity tensor only[38]. This will hold for all planar configurations with an illuminating field invariant in the $x-y$-plane, hence no spatial dispersion occurs which would result in an artificial magnetic response. Substituting the displacements (1) into the definition of the dielectric polarization[39] we can introduce the effective susceptibility tensor $\hat{\chi}(\omega)$

$$\begin{aligned}\mathbf{P}(\mathbf{r},t) &= \eta\sum_{l=1}^{N} q_l\mathbf{r}_l,\\ P_i(\mathbf{r},\omega) &= \epsilon_0\chi_{ij}(\omega)E_j(\mathbf{r},\omega),\end{aligned} \tag{3}$$

where η accounts for the carrier density. This effective susceptibility can be easily calculated. As usual we define the effective permittivity tensor as

$$\hat{\epsilon}(\omega) = \underline{\mathbf{1}} + \hat{\chi}(\omega), \tag{4}$$

that governs the wave propagation of an incident plane wave in an effective medium composed of SRR metaatoms.

Next we consider the possible eigenmodes of Eqs. (1) for the two polarization directions (x or y). It suffices to investigate these two polarizations as long as the system under consideration is linear. In order to describe a SRR with two identical side arms we set $\omega_{01} = \omega_{03} \equiv \omega_{0x}$, $\gamma_1 = \gamma_3 \equiv \gamma_x$, $\sigma_{21} = \sigma_{23} \equiv \sigma$ and $q_1 = q_3 \equiv -q_x$. For the oscillator associated with the SRR base having a different geometry, we put $\omega_{02} \equiv \omega_{0y}$, $\gamma_2 \equiv \gamma_y$ and $q_2 \equiv -q_y$. We note that the latter distinction could have been dropped if the geometry of all constituents of the SRR would have been the same. For the reasons obvious from the consideration below we refrain from doing so.

For a polarization of the incoming plane wave parallel to the x-axis we can solve Eqs. (1) and obtain the following displacements in Fourier domain:

$$\begin{aligned}x_1(\omega) = x_3(\omega) &= -\frac{q_x}{m}\frac{1}{A_x(\omega)}E_x(z,\omega),\\ y_2(\omega) &= 0,\end{aligned} \tag{5}$$

where we have introduced $A_x(\omega) = \omega_{0x}^2 - \omega^2 - i\omega\gamma_x$.

For the polarization in y-direction we obtain

$$\begin{aligned}x_1(\omega) = -x_3(\omega) &= -\frac{q_y}{m}\frac{\sigma}{A_x(\omega)A_y(\omega) - 2\sigma^2}E_y(z,\omega),\\ y_2(\omega) &= -\frac{q_y}{m}\frac{A_x(\omega)}{A_x(\omega)A_y(\omega) - 2\sigma^2}E_y(z,\omega),\end{aligned} \tag{6}$$

with $A_y(\omega) = \omega_{0y}^2 - \omega^2 - i\omega\gamma_y$.

Considering the eigenmodes for x-polarization, we observe that two parallel dipoles ($x_1 = x_3$) are induced, while due to symmetry constraints no dipole is induced in y-direction ($y_2 = 0$), see Fig. 2(c). By contrast, besides a dipole in y-direction the y-polarized illumination induces oscillating dipoles in x-direction in both arms. But due to the anti-symmetric oscillation $x_3 = -x_1$ [Eq. (6)], the dipoles in the SRR arms [Fig. 2(d)] do not radiate into the far-field because they oscillate π out-of-phase and interfere destructively. Hence, no cross-polarization is observed and the far-field polarization equals that of the illumination. Later we will prove that any radiation emerging from cross-polarized dipole moments will result in an optical activity, as expected.

By substituting Eqs. (5, 6) in Eqs. (3) we get the susceptibility tensor for the pertinent SRR configuration

$$\begin{aligned}\hat{\chi}(\omega) &= \begin{pmatrix}\chi_{xx}(\omega) & 0 & 0\\ 0 & \chi_{yy}(\omega) & 0\\ 0 & 0 & 0\end{pmatrix},\\ \chi_{xx}(\omega) &= \frac{q_x^2\eta}{m\epsilon_0}\frac{2}{A_x(\omega)},\\ \chi_{yy}(\omega) &= \frac{q_y^2\eta}{m\epsilon_0}\frac{A_x(\omega)}{A_x(\omega)A_y(\omega) - 2\sigma^2},\end{aligned} \tag{7}$$

with the polarization $\mathbf{P} = -\eta\ (q_x(x_1 + x_3), q_y y_2, 0)^T$, according to Eq. (3). As expected, the susceptibility tensor is diagonal. Hence, the eigenmodes of the effectively homogenous medium are linearly polarized and orthogonal. Due to the polarization dependent carrier dynamics the SRR shows a linear dichroitic behavior. Hence, our model correctly predicts the linear polarization eigenstates as required by the mirror-symmetry with respect to the $x-z$-plane. The only unknown parameters are those describing the oscillators and their coupling strengths. They can be determined by matching

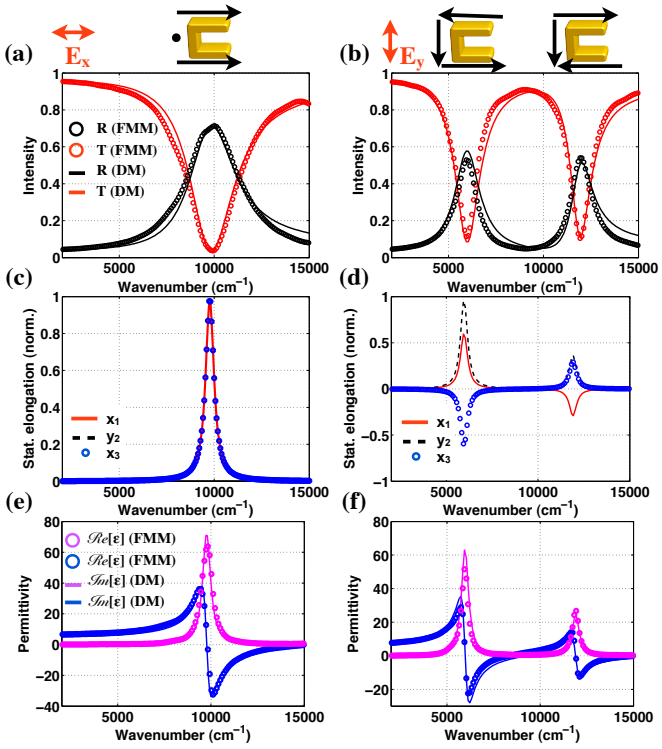

FIG. 2. (Color online) The rigorously calculated (FMM) far-field transmission/reflection spectra compared with those obtained by the analytical coupled dipole model (DM) for the two indicated polarization directions [(a) x-polarization and (b) y-polarization]. The stationary carrier elongation (normalized imaginary part of $x_{1,3}$ and y_2) for the two corresponding polarizations [(c) and (d)]. (e),(f) The exactly retrieved parameters compared to the analytical calculations.

the optical coefficients of an effective medium whose permittivity is described by Eqs. (7) to the spectra obtained by rigorous simulations or far-field measurements of the structure.

In order to find the oscillator parameters, we performed numerical Fourier Model Method (FMM) calculations[40] of a periodic array of gold SRR's[41] similar to those reported in Ref. 2. These numerical far-field observables (reflected and transmitted intensities) were fitted by using the effective permittivity tensor Eq. (4) for both polarization directions in a conventional transfer matrix formalism that computes reflection and transmission from a slab of equal thickness[42]. Results are shown in Fig. 2(a) and 2(b).

Once the unknown parameters have been found the frequency dependent stationary elongations of the oscillators can be determined as shown in Figs. 2(c) and (d). They can be used to identify the carrier oscillations of the different plasmonic eigenmodes. These carrier oscillations are shown on top of Fig. (2) and their horizontal position relates to the respective resonance frequency. The observed eigenmodes are documented in literature[38]. Figures 2(e) and (f) show the rigorously retrieved effective material properties together with the ones of the analytical model. Excellent agreement is observed. The rigorous results were obtained by applying a common parameter retrieval based on an inversion of the matrix formalism to calculate the effective parameters on the basis of complex reflected and transmitted amplitudes for a certain slab thickness. We underline that the unknown oscillator parameters can be obtained by comparing the far-field intensity only. The derived effective material parameters are in excellent agreement with the rigorous results, but they were derived without the necessity of knowing the complex-valued fields. This will be advantageous for optical active structures where the experimental determination of these parameters is in general involved (e.g. phase resolved measurements are not required).

III. THE L - METAATOM

As outlined in the introduction low-symmetry metaatoms are investigated in order to reveal new optical phenomena like asymmetric transmission. We will therefore extend the previous considerations towards optically active effective media by rearranging the SRR constituents. In the following we shall rely on the oscillator parameters obtained by the fitting procedure above. Using these parameters in conjunction with the analytical expressions for the rearranged constituents as derived below, the optical response of the modified metaatoms can be predicted. The first investigated structure is the L - metaatom[43,44]. In this geometry one of the SRR arms is omitted in order to prevent the cancelation of the far-field that originated from the antiparallel dipole moments. Hence, it is expected to obtain polarization rotation. To get specific in Eq. (1) one horizontal oscillating dipole, e.g., dipole '3', has to be dropped. Hence, we obtain for x-polarization

$$x_1^x = -\frac{q_x}{m}\frac{A_y(\omega)}{A_x(\omega)A_y(\omega)-\sigma^2}E_x(z,\omega),$$
$$y_2^x = -\frac{q_x}{m}\frac{\sigma}{A_x(\omega)A_y(\omega)-\sigma^2}E_x(z,\omega), \qquad (8)$$

and for y-polarization

$$x_1^y = -\frac{q_y}{m}\frac{\sigma}{A_x(\omega)A_y(\omega)-\sigma^2}E_y(z,\omega),$$
$$y_2^y = -\frac{q_y}{m}\frac{A_x(\omega)}{A_x(\omega)A_y(\omega)-\sigma^2}E_y(z,\omega). \qquad (9)$$

From the resulting polarization Eq. (3)

$$\mathbf{P}^j(z,\omega) = -\eta\begin{pmatrix} q_x x_1^j \\ q_y y_2^j \\ 0 \end{pmatrix}, \; j \in [x,y] \qquad (10)$$

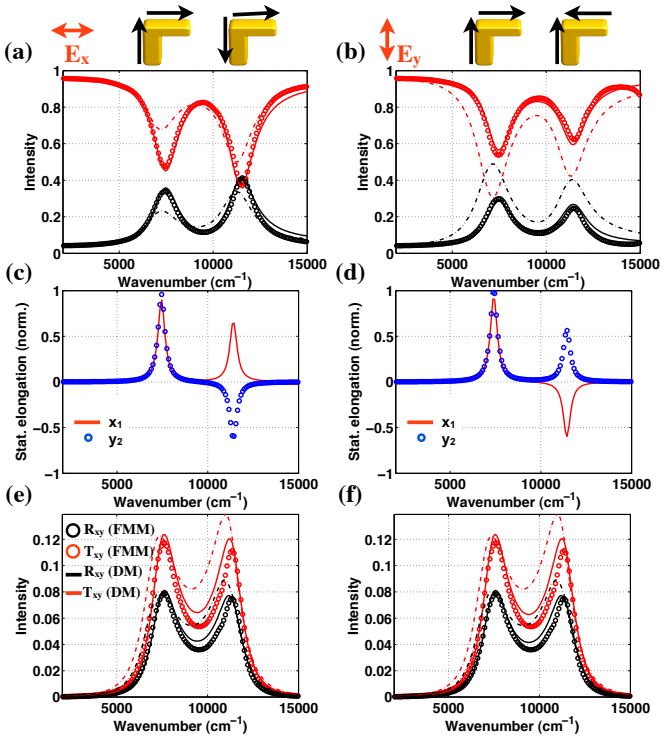

FIG. 3. (Color online) The far-field response of the L - structure for $x-$ (a) and $y-$ polarization (b) . In addition to the numerical (FMM, spheres) and the fitted data (DM, solid lines) the predicted spectra incorporating the SRR parameters (dashed-dotted lines) are plotted. (c),(d) In contrast to the SRR both eigenmodes can be excited for each polarization direction. The respective numerical cross-polarization contributions (FMM, circles) compared with the model predicted (dashed-dotted lines) and the fitted (solid lines) values are shown in (e) and (f). Note that figures (e) and (f) are identical as required for such kind of effective media and are only shown for completeness.

the susceptibility reads as

$$\hat{\chi}(\omega) = \begin{pmatrix} \chi_{xx}(\omega) & \chi_{xy}(\omega) & 0 \\ \chi_{yx}(\omega) & \chi_{yy}(\omega) & 0 \\ 0 & 0 & 0 \end{pmatrix},$$

$$\chi_{xx}(\omega) = \frac{q_x^2\eta}{m\epsilon_0}\frac{A_y(\omega)}{A_x(\omega)A_y(\omega)-\sigma^2},$$

$$\chi_{yy}(\omega) = \frac{q_y^2\eta}{m\epsilon_0}\frac{A_x(\omega)}{A_x(\omega)A_y(\omega)-\sigma^2},$$

$$\chi_{yx}(\omega) = \chi_{xy}(\omega) = \frac{q_xq_y\eta}{m\epsilon_0}\frac{\sigma}{A_x(\omega)A_y(\omega)-\sigma^2}. \quad (11)$$

The most significant change compared to the SRR is the appearance of off-diagonal elements in the susceptibility tensor $\hat{\chi}(\omega)$ which is, however, symmetric leading also to $\varepsilon_{ij}(\omega) = \varepsilon_{ji}(\omega)$. This symmetry relation is important because it is required for time reversal, known as the Onsager-Casimir principle[30–32]. As expected the tensor of the effective permittivity has the same form as that for planar optical active media[18,25] resulting in asymmetric transmission due to elliptical dichroism. Note that the optical response would change dramatically if both arms would be identical. In this case the diagonal elements $\chi_{ii}(\omega)$ are identical too and the tensor can be diagonalized by an rotation of $\pi/4$. So the polarization eigenstates would be linear and the effective medium would be linearly dichroitic. This is clear since the metaatom would have an additional mirror symmetry with respect to the plane defined by the surface normal and the line $x = y$, see Ref. 45.

Another difference while comparing the L - to the SRR metaatom is that the splitting σ between both resonances is reduced (by a factor of $\sqrt{2}$), which follows from dropping one of the SRR arms.

In order to check whether our simple description is valid and to reveal the relation between the SRR and the L - structure eigenmodes, we performed again numerical FMM simulations for the L - metaatom and compared the results to the analytical model in Fig. 3. Since we deal now with more complex effective media where the full tensorial nature of the permittivity tensor has to be taken into account the standard transfer matrix algorithm cannot be applied. Hence, it is challenging to determine the scattering coefficients analytically[46] or even to invert them to retrieve effective parameters directly. Therefore we used an adapted Fourier Modal Method to determine the transmitted and reflected intensities[47]. In a first approximation we used the parameters which we determined for the SRR. Based on these parameters we calculated $\chi_{ij}(\omega)$ and the far-field intensities as shown in Fig. 3(a,b) for the L - structure. The associated eigenmodes for the carriers are shown in Fig. 3(c,d). The curves for both the co-polarized Fig. 3(a,b) and the cross-polarized intensities Fig. 3(e,f) are in good qualitative agreement for the rigorous FMM results (dotted line) and the analytical model (dashed line) based on the previously derived SRR oscillator parameters. Although there are deviations between the actual resonance strength, the agreement, e.g. for the resonance positions, is obvious. Note that the intensities, in particular for the cross-polarized fields, can be solely predicted by the coefficients obtained from the SRR. There, an almost perfect agreement is observed.

In a second step we adapted the oscillator parameters in order to fit the exact calculations [solid lines in Fig. 3(a,b,e,f)] providing an almost perfect coincidence with the numerical values[48]. Note that the fitting is done only for the co-polarized intensities from which the cross-polarized intensities follow.

A last step yields the effective permittivity tensor, that is inherently accessible and already applied in order to fit the spectra in Fig. 4. It can be seen that for the two polarization directions two eigenmodes appear as Lorentz-shaped resonances for the effective permittivities. They differ in strength, due to the different geometrical parameters of the L - arms, Fig. 4(a,b). The off-diagonal elements $\epsilon_{ij}(\omega)$ are identical as discussed before, [Fig. 4(c)]. Considering especially the second resonance for

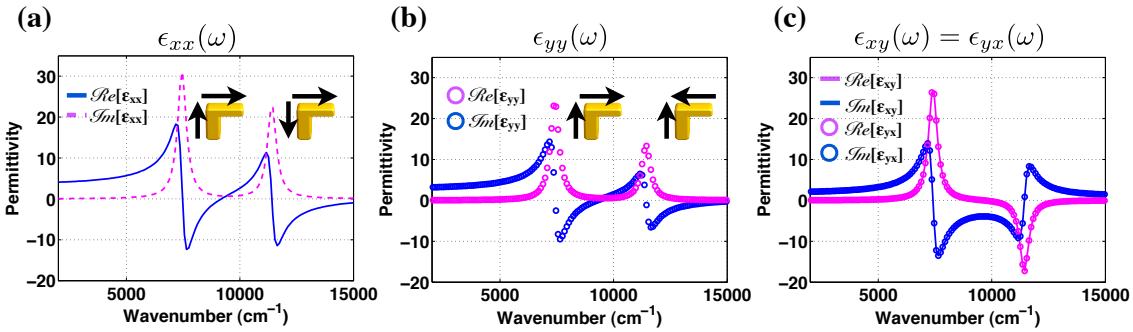

FIG. 4. (Color online) The diagonal effective permittivity tensor elements of the L - metaatom: (a) $\epsilon(\omega)_{\rm xx}$ and (b) $\epsilon(\omega)_{\rm yy}$. The arrows indicate the current flow, given by direction of the carrier oscillation for the particular eigenmode. (c) The off-diagonal elements $\epsilon(\omega)_{ij}$ comprising a Lorentz resonance around $\bar{\nu} = 7,000\ cm^{-1}$ and an anti-Lorentz resonance at $\bar{\nu} = 11,000\ cm^{-1}$.

the off-diagonal tensor elements near $\bar{\nu} = 11,000\ cm^{-1}$, we observe a Lorentzian anti-resonance that might suggest gain within the system due to the negative imaginary part. However, the nature of this resonance can be explained by the introduced formalism as well. Since the permittivity is proportional to the susceptibility Eq. (4) and hence also to the carrier displacements Eqs. (11), a negative sign corresponds to a phase difference of π between both oscillating carrier densities (antiparrallel oscillations), while for the positive Lorentz resonance at around $\bar{\nu} = 7,000\ cm^{-1}$, both are oscillating in-phase [sketched by the arrows in Fig. 4(a)]. Thus, the negative sign in the imaginary part of the permittivity can by fully explained by means of the mutual interplay of the coupled oscillators.

IV. THE S - METAATOM

In order to verify the model we are going to investigate another modification of the SRR, namely the S - structure[49,50] [Fig. 1(a)]. To observe optical activity with the same number of coupled entities as for the SRR its mirror symmetry has to be broken. Therefore one of the SRR arms (e.g. x_3) is turned with respect to the SRR base.

This *opening* of the SRR structure is expected to enable the observation of two modes for x-polarization, since the oscillator in the base (y_2) can now oscillate in-phase or out-of-phase with the two remaining x-oriented oscillators of the S - structure that are excited by the x-polarized electric field. For y-polarization the situation is similar, but now the two oscillators in the horizontal arms (x_1, x_3) are allowed to oscillated in-phase or out-of-phase to the excited oscillator in the base (y_2). Mathematically this modification can be considered by setting $\sigma_{23} = -\sigma_{21} \equiv \sigma$ (see Eq. 1), while all other parameters appear similar to the ones applied for the SRR.

With these initial assumptions, which reflect all modifications to the geometry, the calculations can be repeated in analogy to those for the SRR and the L - structure. Thus, we obtain the elongations for x-polarized excitation

$$x_1^x = x_3^x = -\frac{q_x}{m}\frac{A_y(\omega)}{A_x(\omega)A_y(\omega) - 2\sigma^2}E_x(z,\omega),$$
$$y_2^x = -\frac{q_x}{m}\frac{2\sigma}{A_x(\omega)A_y(\omega) - 2\sigma^2}E_x(z,\omega), \qquad (12)$$

and for y-polarized excitation

$$x_1^y = x_3^y = -\frac{q_y}{m}\frac{\sigma}{A_x(\omega)A_y(\omega) - 2\sigma^2}E_y(z,\omega),$$
$$y_2^y = -\frac{q_y}{m}\frac{A_x(\omega)}{A_x(\omega)A_y(\omega) - 2\sigma^2}E_y(z,\omega), \qquad (13)$$

as well as the respective effective susceptibility tensor

$$\chi(\omega) = \begin{pmatrix} \chi_{xx}(\omega) & \chi_{xy}(\omega) & 0 \\ \chi_{yx}(\omega) & \chi_{yy}(\omega) & 0 \\ 0 & 0 & 0 \end{pmatrix},$$
$$\chi_{xx}(\omega) = \frac{q_x^2\eta}{m\epsilon_0}\frac{2A_y(\omega)}{A_x(\omega)A_y(\omega) - 2\sigma^2},$$
$$\chi_{yy}(\omega) = \frac{q_y^2\eta}{m\epsilon_0}\frac{A_x(\omega)}{A_x(\omega)A_y(\omega) - 2\sigma^2},$$
$$\chi_{yx}(\omega) = \chi_{xy}(\omega) = \frac{q_xq_y\eta}{m\epsilon_0}\frac{2\sigma}{A_x(\omega)A_y(\omega) - 2\sigma^2}. \qquad (14)$$

In Eqs. (14) we have used the polarization Eq. (3) which is found to coincide with that of the SRR structure, whereas the elongations are different. With respect to the splitting of the resonances, we expect the same resonance positions as for the SRR for y-polarization, since 2σ appears in the denominator of the SRR oscillation amplitudes [Eqs. (7) for y-polarization] as well as in all elongations in Eqs. (12) and Eqs. (13).

Performing the respective numerical and analytical calculations as before for the L - structure, we can predict the spectral response as well as the effective material properties based on the plasmonic eigenmodes. The results are shown in Fig. 5.

Considering these eigenmodes in Fig. 5(d,e), we may distinguish two situations. At first an eigenmode which is represented by three dipoles being in phase along the entire structure. The second eigenmode is characterized by

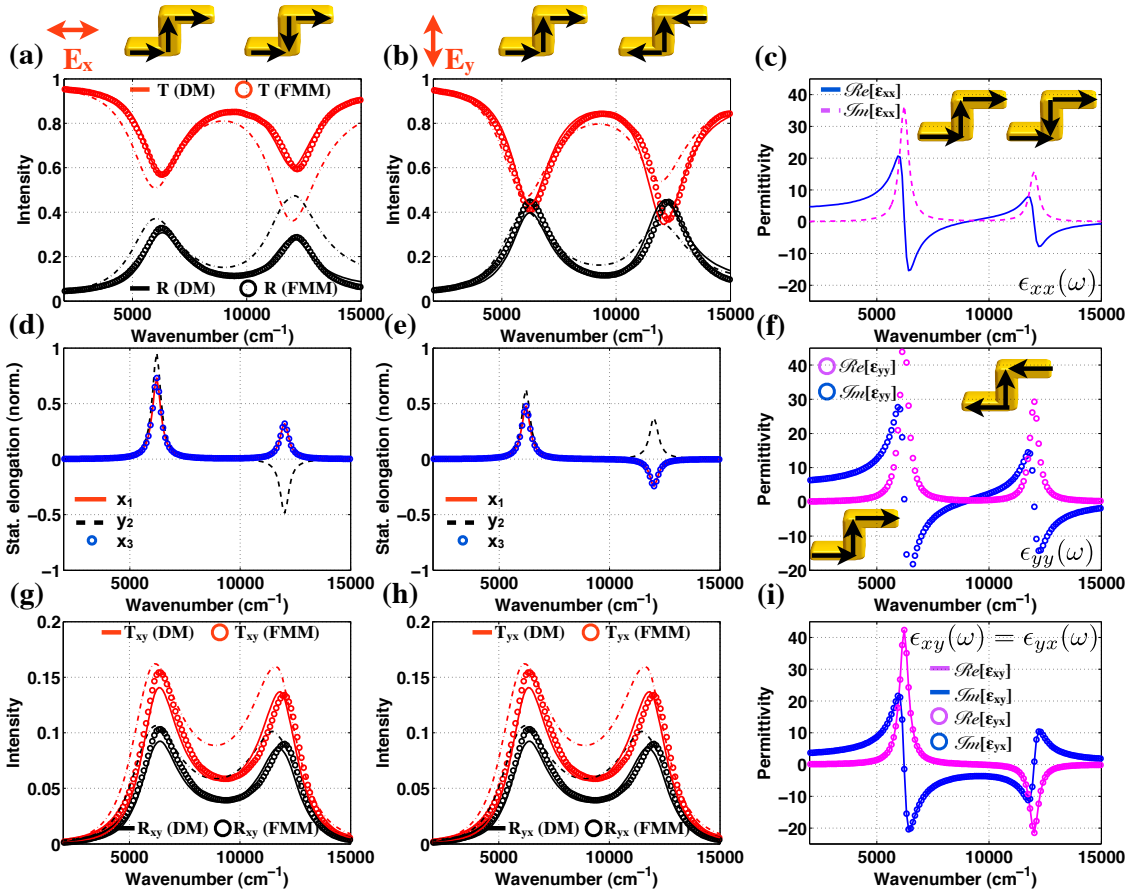

FIG. 5. (Color online) The far field spectra of the S - structure (a) x-polarization and (b) y-polarization obtained by numerical simulations (circles), predictions based on the SRR structure parameters (dashed-dotted lines), and adapting the parameters to fit the numerical values (solid lines). The carrier eigenmodes, i.e., an in line current over the entire structure and antiparallel currents [normalized imaginary part of $x_1(\omega), y_2(\omega), x_3(\omega)$] with respect to the center part of the S - structure are observed for the two polarization directions (d) x and (e) y. The comparison between the cross-polarization contributions (T_{ij}, R_{ij}) for the numerical simulations (circles), the predicted lines from the SRR parameters (dashed-dotted lines) and the fitted parameter spectra (solid lines) for the found parameters deduced for fitting the co-polarized response (T_{ii}, R_{ii}). The effective permittivity tensor diagonal (c), (f) and the off-diagonal components (i).

two dipole being in-phase in the arms and out-of-phase in the base. Both eigenmodes are excited for x- and y-polarization, respectively, and will lead to spectral resonances appearing as dips and peaks in transmission or reflection, respectively [Fig. 5(a,b)]. The spectral positions of the resonances are in agreement with the expectations from the SRR structure resonances.

As expected, for both the S - and the L - metaatom the in-phase eigenmodes appear at smaller wavenumbers (larger wavelengths) compared to the out-of-phase ones. This is completely in agreement with arguments from plasmon hybridization theory[51].

Again the use of the oscillator parameters as optimized for the SRR structure [dash-dotted lines in Fig. 5(a,b,g,h)] reveals the relationship between both structures, since the numerically (circles) calculated spectra agree with respect to the overall shape and the resonance positions Fig. 5(d,e) very well with the analytical predictions (solid and dashed lines). A subsequent fitting again improves the results towards almost excellent agreement, which can also be observed for the cross- polarization observables Fig. 5(g,h). Considering the tensor components of the effective permittivity, we observe a difference between the diagonal entries due to the geometrical differences in the S - structure center and arms, while the anti-resonance for the out-of-phase eigenmode is observed in the off-diagonal elements with the same origin as discussed for the L-structure.

Finally we provide all parameters required for the analytical calculations presented here for the SRR as well as the two presented modifications in Tab. I.

V. SUMMARY

In summary, we have presented an analytical model which permits the calculation of effective material parameters for planar metamaterials consisting of variable

TABLE I. The fitted oscillator parameters applied to reproduce the optical far-field intensities for the SRR as well as the adapted parameters for the L- and S- structure are presented. For consistence with the corresponding figures, all spectral units are given in wavenumber units (cm^{-1}).

Fitting parameter	SRR	L	S
ω_{0x}, ω_{0y} $[cm^{-1}]$	9770, 9050	9770, 9500	9770, 9350
γ_x, γ_y $[cm^{-1}]$	520, 420	520, 420	520, 420
$\sqrt{\sigma}$ $[cm^{-1}]$	6100	6100	6100
$q_x^2\eta/\epsilon_0 m$ $[AsV/m^2Kg]$	$0.65 \cdot 10^{39}$	$0.83 \cdot 10^{39}$	$0.35 \cdot 10^{39}$
$q_y^2\eta/\epsilon_0 m$ $[AsV/m^2Kg]$	$1.1 \cdot 10^{39}$	$0.55 \cdot 10^{39}$	$1.10 \cdot 10^{39}$

metaatoms formed by a few straight wire sections of potentially different shape. The model takes advantage of resonant electric dipole oscillations in the wires and their mutual coupling. The pertinent form of the metaatom determines the actual coupling features. Thus this model represents a kind of building block approach for quite different metaatoms. Once the constants describing the respective dipole oscillations for one particular arrangement have been determined, where here the SRR has been used, the properties of another, modified metaatom can be easily predicted. Since in particular the effect of asymmetric transmission for circular polarized light attracted a lot of research interest recently, we focused here on planar metaatoms that are optically active. Within our model all properties of the effective material tensors for such kind of media are correctly predicted and the corresponding scattering characteristics are in very good agreement with the rigorous numerical results.

VI. ACKNOWLEDGEMENTS

Financial support by the Federal Ministry of Education and Research (ZIK, MetaMat) as well as from the State of Thuringia within the ProExcellence program is acknowledged.

* joerg.petschulat@uni-jena.de
† also with: Fraunhofer Institute of Applied Optics and Precision Engineering Jena, Germany.

[1] U. K. Chettiar, A. V. Kildishev, H.-K. Yuan, W. Cai, S. Xiao, V. P. Drachev, and V. M. Shalaev, Opt. Lett. **32**, 1671 (2007).
[2] G. Dolling, M. Wegener, C. Soukoulis, and S. Linden, Opt. Lett. **32**, 53 (2007).
[3] J. Valentine, S. Zhang, T. Zentgraf, G. B. E Ulin-Avila, Dentcho A. Genov, and X. Zhang, Nature **455**, 376 (2008).
[4] J. Valentine, J. Li, T. Zentgraf, G. Bartal, and X. Zhang, Nature Mat. **8**, 568 (2009).
[5] A. Alù and N. Engheta, Phys. Rev. Lett. **102**, 233901 (2009).
[6] Y. Lai, J. Ng, H. Y. Chen, D. Z. Han, J. J. Xiao, Z.-Q. Zhang, and C. T. Chan, Phys. Rev. Lett. **102**, 253902 (2009).
[7] M. Farhat, S. Guenneau, and S. Enoch, Phys. Rev. Lett. **103**, 024301 (2009).
[8] Justice, S. Cummer, J. Pendry, and A. Starr, Science **314**, 977 (2006).
[9] U. Leonhardt, Science **312**, 1777 (2006).
[10] E. E. Narimanov and A. V. Kildishev, Appl. Phys. Lett. **95**, 041106 (2009).
[11] S. M. Vukovic, I. V. Shadrivov, and Y. S. Kivshar, Appl. Phys. Lett. **95**, 041902 (2009).
[12] D. Ö. Güney and D. A. Meyer, Phys. Rev. A **79**, 063834 (2009).
[13] N. Papasimakis, V. A. Fedotov, N. I. Zheludev, and S. L. Prosvirnin, Phys. Rev. Lett. **101**, 253903 (2008).
[14] N. Liu, L. Langguth, J. K. Thomas Weiss and, M. Fleischhauer, T. Pfau, and H. Giessen, Nature Materials **8**, 758 (2009).
[15] C. Helgert, C. Menzel, C. Rockstuhl, E. Pshenay-Severin, E. B. Kley, A. Chipouline, A. Tünnermann, F. Lederer, and T. Pertsch, Opt. Lett. **34**, 704 (2009).
[16] C. García-Meca, R. Ortuño, F. J. Rodríguez-Fortuño, J. Martí, and A. Martínez, Opt. Lett. **34**, 1603 (2009).
[17] M. Thiel, G. von Freymann, S. Linden, and M. Wegener, Opt. Lett. **34**, 19 (2009).
[18] B. Bai, Y. Svirko, J. Turunen, and T. Vallius, Phys. Rev. A **76**, 023811 (2007).
[19] L. Arnaut, J. Electromagn. Waves Appl. **11**, 1459 (1997).
[20] J. A. Reyes and A. Lakhtakia, Opt. Comm. **266**, 565 (2006).
[21] S. Prosvirnin and N. Zheludev, J. Opt. A: Pure Appl. Opt. **11**, 074002 (2009).
[22] S. Tretyakov, I. Nefedov, A. Shivola, S. Maslovski, and C. Simovski, J. Electromagn. Waves Appl. **17**, 695 (2003).
[23] V. A. Fedotov, P. L. Mladyonov, S. L. Prosvirnin, A. V. Rogacheva, Y. Chen, and N. I. Zheludev, Phys. Rev. Lett. **97**, 167401 (2006).
[24] V. Fedotov, A. Schwanecke, and N. Zheludev, Nano Lett **7**, 1997 (2007).
[25] S. V. Zhukovsky, A. V. Novitsky, and V. M. Galynsky, Opt. Lett. **34**, 1988 (2009).
[26] J. Pendry, Science **306**, 1353 (2004).
[27] S. Tretyakov, A. Sihvola, and L. Jylhä, Photonics Nanostruct. Fundam. Appl. **3**, 107 (2005).
[28] J. Zhou, J. Dong, B. Wang, T. Koschny, M. Kafesaki, and C. M. Soukoulis, Phys. Rev. B **79**, 121104(R) (2009).
[29] J. Petschulat, C. Menzel, A. Chipouline, C. Rockstuhl, A. Tünnermann, F. Lederer, and T. Pertsch, Phys. Rev. A **78**, 043811 (2008).
[30] L. Onsager, Phys. Rev. **37**, 405 (1931).
[31] H. Casimir, Rev. Mod. Phys. **17**, 343 (1945).
[32] S. Tretyakov, A. Sihvola, and B. Jancewicz, J. Electromagn. Waves Appl. **16**, 573 (2002).
[33] J. Petschulat, A. Chipouline, A. Tünnermann, T. Pertsch, C. Menzel, C. Rockstuhl, and F. Lederer, Phys. Rev. A **80**, 063828 (2009).
[34] H. Raether, *Surface plasmons* (Springer, New York, 1988).

[35] S. Tretyakov, *Analytical Modeling in Applied Electromagnetics* (Artech House, Boston, 2003).

[36] P. S. Pershan, Phys. Rev. **130**, 919 (1963).

[37] N. Liu, H. Liu, S. Zhu, and H. Giessen, Nature Photonics **3**, 157 (2009).

[38] C. Rockstuhl, T. Zentgraf, E. Pshenay-Severin, J. Petschulat, A. Chipouline, J. Kuhl, T. Pertsch, H. Giessen, and F. Lederer, Optics Express **15**, 8871 (2007).

[39] R. E. Raab and O. L. D. Lange, *Multipole Theory in Electromagnetism* (Clarendon, Oxford, 2005).

[40] L. Li, J. Opt. Soc. Am. A **14**, 2758 (1997).

[41] The period in x- and y-direction is 0.4 μm, the SRR arm length 0.2 μm, the base width 0.08 μm, the arm width 0.04 μm and the metal film thickness 0.025 μm. Gold material parameters were taken from literature[52]. As a substrate index we used $n_{\mathrm{sub}} = 1.5$ and for the ambient material $n_{\mathrm{amb}} = 1$.

[42] P. Yeh, *Optical Waves in Layered Media* (Jon Wiley & Sons, 1998).

[43] B. Canfield, S. Kujala, M. Kauranen, K. Jemovs, T. Vallius, and J. Turunen, Appl. Phys. Lett. **86**, 183109 (2005).

[44] B. Canfield, S. Kujala, K. Jefimovs, and T. Vallius, J. Opt. A: Pure Appl. Opt. **7**, 110 (2005).

[45] M. Decker, S. Linden, and M. Wegener, Opt. Lett. **34**, 1579 (2009).

[46] G. Borzdov, J. Math. Phys. **38**, 6328 (1997).

[47] L. Li, J. Opt. A: Pure Appl. Opt. **5**, 345 (2003).

[48] We mention that the fitting procedure can be manually performed since the parameters are distinct with respect to their spectral effect, e.g. resonance frequency (ω_0), resonance splitting (σ), resonance width (γ) and resonance strength ($q^2\eta/\epsilon_0 m$).

[49] H. Chen, L. Ran, J. Huangfu, X. Zhang, K. Chen, T. M. Grzegorczyk, and J. A. Kong, Appl. Phys. Lett. **86**, 151909 (2005).

[50] H. S. Chen, L. X. Ran, J. T. Huangfu, X. M. Zhang, and K. S. Chen, Prog. Electromagn. Res. **51**, 231 (2005).

[51] E. Prodan, C. Radloff, N. Halas, and P. Nordlander, Science **302** (2003).

[52] P. B. Johnson and R. W. Christy, Phys. Rev. B **6**, 4370 (1972).